Technical Report

Dylan Patterson
Jonna Jämte
Karl Asklund
Lucas Sevelin
Martin Ling
Theodor Vallgren

December 13, 2023

Version 2.0

LINKÖPING UNIVERSITY

Status

Reviewed	Martin Ling	2023-11-30
Approved	Lars Eriksson	2023-12-13

Project Identity

Group E-mail: tsrt10-evap@groups.liu.se

Homepage: https://tsrt10.gitlab-pages.liu.se/2023/aurobay

Orderer: Lars Eriksson, Linköpings universitet
Phone: +46 (0)13-28 44 09
E-mail: lars.eriksson@liu.se

Customer: Fredrik Wemmnert, Aurobay
Phone: N/A
E-mail: fredrik.wemmert@aurobay.com

Supervisor: Oskar Lind Jonsson
Phone: N/A
E-mail: oskar.lind.jonsson@liu.se

Course Responsible: Daniel Axehill
Phone: +46 (0)13-28 40 42
E-mail: daniel.axehill@liu.se

Participants of the group

Name	**Responsible**	**E-mail**
Dylan Patterson	Responsible for the quality (QS)	dylpa851@student.liu.se
Jonna Jämte	Responsible for the testing (TST)	jonja121@student.liu.se
Karl Asklund	Responsible for the Documentation (DOC)	karas744@student.liu.se
Lucas Sevelin	Responsible for software (SWR)	lucse807@student.liu.se
Martin Ling	Project leader (PL)	marli498@student.liu.se
Theodor Vallgren	Responsible for the design (DES)	theva365@student.liu.se

ABSTRACT

The automotive industry is continuously growing, and even though the trend today is moving towards fossil-free vehicles there is still a big market for gasoline-powered vehicles. The gasoline in those vehicles will evaporate over time, and this gas has to be captured to maintain low emissions. This is done by transporting the gasoline vapours into a canister filled with activated carbon. The active carbon adsorbs the fuel vapours and prevents them from entering the atmosphere. When driving the vehicle these fuel vapors are purged and used for combustion. The purge utilizes the negative pressure in the intake manifold to desorb and transfer the fuel vapour to the engine. However, today there is no existing method to accurately predict the amount of fuel vapours purged from the canister, something this project aims to further investigate.

The project is done as part of the course TSRT10 at Linköpings University in collaboration with Aurobay, a course corresponding to nine ECTS for six students. Initially, a smaller literature study was performed to investigate existing studies on the field and find challenges that may occur.

The first task was to create a setup to collect real-world data from a carbon canister during purge. This was done using a small setup with a vacuum pump, a carbon canister filled with butane and a control system connected to a computer. The data collection was done using an Arduino, with up to 12 temperature sensors connected, one flow meter, and one pressure meter. The data was sent to a Raspberry Pi for storage and later analyzed using MATLAB. For verification of the results, a scale was also used to measure the mass of the canister.

With the data recorded a model could be created. Several models were evaluated, and in the end, one model based on the estimation of fuel concentration for the calculation of the mass change was presented. After analyzing the result this model was further extended using a black-box method to better capture the dynamics of the systems. The model has two design parameters, these can be found using a least squares method for a constant airflow. For varying airflow, the least squares method can not find a good set of parameters, and therefore a mapping of constant airflow and their corresponding parameters are presented.

The result is that no model is perfect, but with proper tuning, the results have been promising for the scenarios tested. Future work could improve on the data collection, create a more precise laboratory setup and investigate how a Kalman filter can be used to better predict the design parameters.

CONTENTS

LIST OF FIGURES

LIST OF TABLES

NOMENCLATURE

Physics constants

ρ_a	Density of air	1293 g/m^3
R	Ideal gas constant	8.314 $J/K \cdot mol$

Design parameters

A	Antoine equation parameter	–
B	Antoine equation parameter	–
C	Antoine equation parameter	–
E	Characteristic energy of adsorption	J/mol
n	Dubinin-Astakhov adsorption parameter	–
V_{can}	Canister volume	m^3

Parameters

$\dot{m}_a$	Mass flow of air	m^3/s
$\dot{m}_{can}$	Mass flow of butane	m^3/s
θ	Fractional coverage	–
BV	Bed volume	–
c	Concentration	–
m_{can}	Mass of butane	g
p	Canister pressure	bar
p_s	Saturated pressure	bar
T	Temperature	K
ΔT	Change between ambient and canister temperature	K

DOCUMENT HISTORY

Version	Date	Changes made	Sign	Reviewer
0.1	2023-11-30	First draft.	Martin Ling	Lars Eriksson
1.0	2023-12-11	Final revision	Martin Ling	Lars Eriksson
2.0	2023-12-13	Approved at BP6	Martin Ling	Lars Eriksson

1 INTRODUCTION

In the ever-evolving landscape of environmental consciousness, the automotive industry finds itself at a critical crossroads, facing the formidable challenge of adapting to increasingly stringent emission regulations. As concerns about climate change intensify, governments around the world are tightening the reins on carbon emissions, placing a particular spotlight on vehicles with combustion engines—the traditional workhorses of our roadways [1]. Though the usage of fossil fuels is steadily decreasing in Sweden according to [2] there is still a long way to go in terms of optimization.

One thing that one may not think about regarding emissions from cars with combustion engines is the vaporization of the fuel. These hydrocarbons (typically petrol) evaporate above $-40°C$ which means at all times in most places on earth. This vapour is extremely toxic to both humans and the environment. There will also be a waste of resources if the vapour is released into the environment without passing the engine first. The solution to this is using a canister containing activated carbon. The activated carbon captures the toxic hydrocarbons and stores them until the purge valve is opened and it flows into the engine.

1.1 Parties

The project is done as a part of the course *TSRT10* at Linköping University, and is done in collaboration with *Aurobay*. See above mentioned contact details and list of all parties.

1.2 Background

Due to its volatility, gasoline evaporates in the tanks of a vehicle. To prevent over-pressure in the tank and allow the evacuation of vapours during refuelling, these vapours must be vented. The hydrocarbon content in the vapours is hazardous to both health and the environment and cannot be released freely into the atmosphere. To prevent this, the EVAP system exists.

The vapors are directed to a carbon canister where they are adsorbed. There is a limit to how much hydrocarbons the filter can adsorb before leakage occurs, therefore the canister must be periodically emptied. This is done by directing a purge airflow from the surroundings through the canister and into the engine's intake manifold, the hydrocarbons are later sent into the cylinders and are then combusted.

To minimize emissions, the capacity of the carbon canister should be kept large, i.e., maximizing the amount of adsorbed hydrocarbons in the canister. The purge airflow is driven by the pressure difference between the surroundings and the intake manifold, and depending on current pressure conditions, there is a limit to when the maximum purge airflow can be generated.

To meet the emission requirements, a gasoline engine has a three-way catalyst. For the three-way catalyst to function, there must be a stoichiometric combustion of gasoline in the engine. Therefore, it is important for the engine's control to correctly manage the air and fuel flow. The purge airflow through the carbon canister will carry both ambient air and hydrocarbons, which must be accounted for in the air-fuel mixture the engine needs.

Currently, it is not possible to directly measure the exact hydrocarbon flow from the EVAP system, so it must be estimated. There is also a safety aspect in the control where the EVAP flow must not constitute too large a part of the total air and fuel flow to the engine.

1.3 Aim and purpose

The purpose of this project is to investigate the purging of a charcoal canister. This would improve the process and thus help the customer Aurobay to release a better product for their customers. Aurobay can thus stay at the forefront of market-leading technology, improving the customer's economy. The specific long-term goal is to examine and improve the purging process of the charcoal canister, which can enhance the overall emissions of the system it is installed on.

The short-term objectives for this project are therefore as follows, to achieve the aforementioned long-term goals:

1. Commission laboratory equipment.
2. Model the hydrocarbon flow from the carbon canister to the intake manifold.
3. Regulate the EVAP flow for an arbitrary purging cycle.
4. If possible, design a regulator to control the purging cycle of the charcoal canister while maintaining flow requirements.
5. If possible, demonstrate the EVAP system in the university's engine test cell.

1.4 Use

The goal for usage is that Aurobay can use the results from this project and implement these on their systems. Furthermore, this can then be utilized by Aurobay customers.

2 THEORY

A brief literature study was combined with initial experiments to create a better understanding of the system. In this chapter, the canisters are briefly explained, together with some theory behind the data acquisition system and finally an introduction to the equations used in the model.

2.1 Canister

The canister needs to be made of a material that can withstand large temperature differences. This is due to the large and rapid change of temperature in the canister during purge and filling. The temperature of the canister increases while filling and decreases while purging, creating a large temperature difference between the canister and the surrounding air [3]. However, the choice of material for the canister is outside the scope of this report.
In different parts of the world, there are different regulations regarding the size of the canister. For example, in the USA the canister is bigger than the canisters need to be in Europe. This is due to that in Europe the petrol stations have an extra ventilation line in the nozzlehead [4]. This ventilation collects the vapours of hydrocarbons instead of letting the canister handle it. In the USA there is no such ventilation system at gas stations. This means that the canisters in the USA must be kept larger to be able to capture the full amount of vapours that form during refuelling.

The canister is separated into two chambers as can be seen in fig. 1. These two chambers are filled with granulates of activated carbon, which will adsorb the fuel vapours coming from the fuel tank. This simple design allows the air from the atmosphere to reach all granules during the purge. This is demonstrated to the right in fig. 1.

As can also be seen in fig. 1 the connection port from the tank and the port to the engine are placed next to each other. One problem that comes with this is that there can be very high concentrations of hydrocarbons just inside the "to engine" port. This makes it harder to predict the amount of hydrocarbons released while purging, and is later sent into the engine. This phenomenon is outside the scope of this report since there is a lack of equipment that can fill the canister at the same time as it's purging.

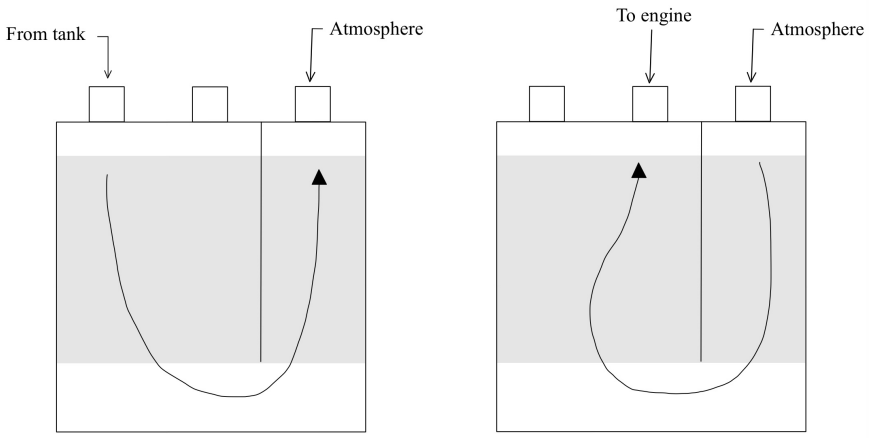

Figure 1: Cross-section for a canister with ports to the engine, from the tank, and the atmosphere.

The activated carbon inside the two chambers is packed together with the help of the two springs which can be seen in fig. 2, one spring for each chamber.

Figure 2: Canister seen from below with springs that keep the active carbon packed inside the canister. The bottom piece of the canister is missing in this picture.

2.2 Activated carbon

The carbon canister is filled with small granulates of activated carbon. The activated carbon is used in many other applications, such as the removal of odour, taste, or filtrating fluids and gas passing through the activated carbon [5]. The porous crystalline structure of the active carbon determines the adsorption capability of the active carbon but is also heavily influenced by the chemical structure. According to Cao et. al. [6], one gram of activated carbon can have up to $2700m^2$ of surface area, but more common values are around $1000 - 1500m^2/g$. The main binding in the active carbon is the van der Waals force and mainly the London force, which attracts the gas and enables the storage capacity of the active carbon. This binding force is a dispersion force acting between adjacent atoms and creates an attractive force, which is utilized in the activated carbon [7].

During a purge cycle, the goal is to make the hydrocarbons flow from the canister to the engine. To do so, it is required that the hydrocarbons undergo desorption from the activated carbon. This is enabled by the airflow through the canister "ripping" the hydrocarbons off the surface of the activated carbon. When doing this, energy is required to break the bond and therefore conserve the energy. The energy used to break the bond is mainly molecular kinetic energy, and therefore the temperature within the canister decreases as a purge cycle is executed. This can be of great use to determine a model for how much hydrocarbons exit the canister.

It has been seen from research that the whole amount of adsorbed hydrocarbons cannot be recovered through desorption[8]. The residuals stuck in the carbon are referred to as "heel". Because of this "heel" the canister can not be completely emptied. The same study also noticed through experiments that both the adsorption and desorption are temperature-dependent. At lower temperatures, the adsorption is more effective, however for lower temperatures desorption is less effective. Thus, at lower temperatures, the charcoal canister generally holds more hydrocarbons.

The granulates are poured into the canister as can be seen in fig. 3.

Figure 3: Canister containing activated carbon separated from the bottom. The spring and plate compressing the active carbon can be seen to the left and the activated carbon in the right chamber.

2.3 Data acquisition

In this section, the essential components required for effective data collection are explained. Particularly, specifications for the Arduino Nano 33 IoT, Raspberry Pi 3B+, the I^2C protocol, and the sensors.

2.3.1 *Arduino Nano 33 IoT*

The Arduino Nano 33 IoT is a cheap and easy-to-use microcontroller with WiFi and Bluetooth connection built in. It comes with 30 GPIO pins, some of which support digital read and write and some analogue read and write. The device is usually powered via the micro USB port, and using that method together with some minor modifications the device can output up to 5V on any of the pins. The device only accepts up to 3.3V as input on the GPIO pins. [9]

2.3.2 *Raspberry Pi 3B+*

The Raspberry Pi 3B+ is a compact single-board computer. It features a powerful 64-bit quad-core processor running at 1.4GHz. Notable features include WiFi, Bluetooth connectivity, and Ethernet. With 40 GPIO pins, the Raspberry Pi provides plenty of connectivity options for hardware components. Its multimedia capabilities, SD card support, and compact form factor make it a versatile choice for a variety of computing tasks. [10]

2.3.3 *I2C*

I^{2}C (sometimes denoted as I2C) is a protocol used to communicate between several micro-controllers. The protocol has the major benefit of requiring only four wires between the controller and a sensor, more sensors can be added by daisy-chaining the sensors. The unit receiving data is usually denoted as Master and the senders as Slaves [11]. The protocol requires power and ground on two of the lines, the remaining two are SDA and SCL respectively. SCL is the clock line, this is used to prohibit data transmission while the master is occupied receiving data from another slave. SDA is used to transmit the data. [12, 13]

2.3.4 *Sensors*

A sensor detects and responds to physical inputs and its primary function is to convert these physical phenomena, such as pressure, temperature, and flow, into measurable signals that can be interpreted. The sensors used for this project are temperature sensors, flow sensors, and a pressure sensor, see fig. 4. The temperature and flow sensors are connected to the Arduino using I^{2}C , while the pressure sensor is connected to an analogue read GPIO pin on the Arduino.

(a) Temperature sensor

(b) Pressure sensor

(c) Mass flow sensor

Figure 4: Different types of sensors used in the project.

Specification datasheet for the sensors in fig. 4 is presented in table 1.

Table 1: Sensor specifications.

Sensor type	**Pressure**	**Temperature**	**Flow**
Name	Piezoresistive (PR) differential pressure transmitters for harsh environments, Kistler 4264A	Kmeter Isolation Unit with Thermocouple Temperature Sensor (MAX31855)	Sensirion SFM3000-200-C
Measurement unit	bar	°C	l/m
Operating range	± 0.17	-200 - 1350 °C	± 200 l/m
Limit	0.51 bar	N/A	1 bar
Resolution	N/A	0.25 °C	N/A
Accuracy	0.1%	± 2%	± 1.5%
Electrical interface	0-5V Analog signal	I^2C	I^2C
Physical interface	M10x1 male	N/A	⌀ 19mm Hose

2.4 Modeling

The initial model of the hydrocarbon mass flows out of the canister during the purge. Lars Eriksson introduced eq. (1) as an initial estimate of how to model the behaviour of the carbon canister.

$$\dot{m}_{can} = -\alpha \cdot \dot{m}_a \cdot m_{can} \tag{1}$$

Where $\dot{m}_{can}$ is the mass flow of hydrocarbons from the canister, α is an unknown constant, $\dot{m}_a$ is the mass-airflow during the purge and m_{can} is the mass of the remaining hydrocarbons in the canister. This did however not capture the exponential behavior of the mass change.

Another equation, proposed by Zaremba et. al. [14] utilizes that we can measure the mass difference and the flow to give eq. (2).

$$\dot{m}_{can} = \Delta m_{can} + \rho_a(BV) \cdot V_{can} \tag{2}$$

Where V_{can} is the canister volume, $= 1.5$ L for an EU canister. This is further simplified with the assumption that the density of air is constant throughout the cycle. This is of course not true, but it greatly simplifies the modelling and the variation of density is assumed small. Furthermore, the mass of butane is not known, and cannot be measured with the current equipment.

Based on eq. (2), the idea is to convert the mass flow to mass and then multiply it by an estimate of the butane concentration to get the mass change of butane. This is made since there exists no way of measuring the mass change of butane with the existing equipment. Instead, it is only possible to measure the total change of mass. See eq. (3).

$$\dot{m}_{can} = c \cdot \rho_a \cdot \dot{m}_a \tag{3}$$

Where c is the concentration of butane. This assumes that the concentration increases by adsorption when the concentration is below equilibrium and decreases for concentrations larger than equilibrium. A better approach is to use the fractional coverage of adsorbate, [15] resulting in eq. (4).

$$\dot{m}_{can} = k_1 \cdot \theta \cdot \rho_a \cdot \dot{m}_a \tag{4}$$

Where k_1 is a parameter used for scaling and is determined through experimentation. The fractional coverage can not be measured, it must be calculated. Calculating θ is done using the Dubinin–Radushkevich equation [16], as in eq. (5).

$$\theta = exp\Big[-\Big(\frac{RTln\frac{p_s}{p}}{E}\Big)^n\Big] \tag{5}$$

Where n and E are scalars that have to be determined using experiments. Östermark [15] found through experimentation that $n = 1.43$ and $E = 18422$ are good fits.

Lastly, p_s is calculated according to the Antoine equation [17] described in eq. (6).

$$\log_{10}(p_s) = A - \frac{B}{T - C} \tag{6}$$

Where all parameters except T are dependent on the temperature and type of gas. It should be noted that the saturated pressure is always higher than the pressure in the canister, otherwise, imaginary solutions of θ, from eq. (5), are obtained. The values of the constants A, B and C are acquired from the National Institute of Standards and Technology [18] and are presented in table 2.

Table 2: Parameter values for butane in different temperatures.

Temperature interval [K]	A	B	C
195.11 - 272.81	3.85002	909.65	-36.146
272.66 - 425	4.35576	1175.581	-2.071

3 METHOD

To create a model for the system data needed to be collected. This was done using a test bench and measuring system for a carbon canister. For all experiments, the gasoline vapours were replaced with butane as it is easier to handle but has similar properties.

3.1 Test bench for data collection

A test bench provided by Aurobay with a control system was used to purge the carbon canisters. The system consists of a cart, housing a grey box featuring hose connections, a computer that controls the system, and a vacuum pump to create a flow in the carbon canister.

The test bench is equipped with a flow sensor out of the canister, that also acts as a valve, which is controlled by the system provided by Aurobay. The computer on the test bench runs a simple controller, which uses the flow out from the canister as a control parameter. The controller software requires the flow at every second as input from the user, allowing the user to specify the flow cycle, such as FTP75 or a constant flow. The length of the cycle is also specified with the flow. The software can log the measurements for the flow out of the canister and output it in an Excel file.

3.2 Measuring system for data collection

A laboratory setup was assembled for use in the experiments, alongside the test bench from Aurobay. The setup incorporates several temperature sensors, specifically KMeterISO units from M5stack, connected using I^2C . Flow into the canister is monitored with an SFM3000 sensor from Sensirion, connected via I^2C . Additionally, a Kistler 4264A pressure sensor is integrated, and connected to an analogue input on the Arduino. The inclusion of a heavy-load scale, Precision Balance MS32001L/01, enables the recording of the canister's weight by connecting it to a computer via USB. Data from the sensors are collected using an Arduino Nano 33 IoT, which is connected to a Raspberry Pi 3B+ via a USB cable. The Raspberry Pi is employed to organize the data and store it in a CSV file, facilitating later access in MATLAB for processing.

A picture of the data collection setup is shown in fig. 5. The connections, from the Arduino to the hub and pressure sensor connector, are as follows in fig. 6. The order in which the sensors are connected to the I^2C -hub is not of importance since the communication with each sensor is done via their unique ID number.

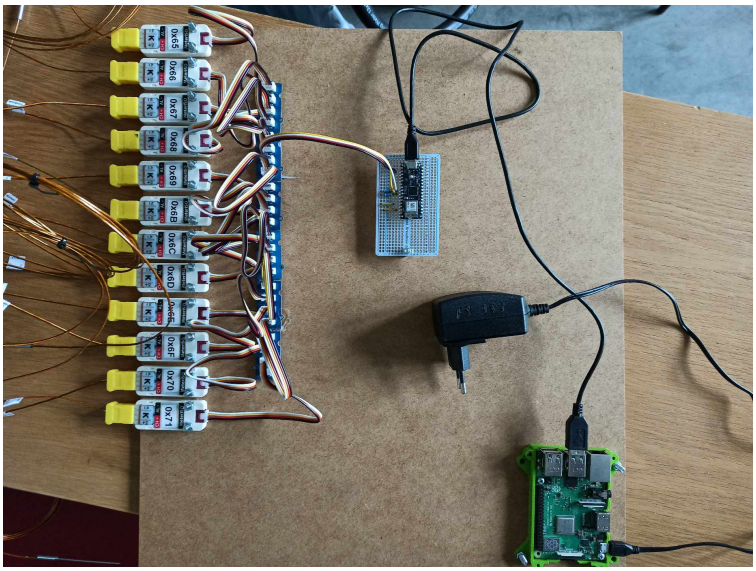

Figure 5: Measuring system setup.

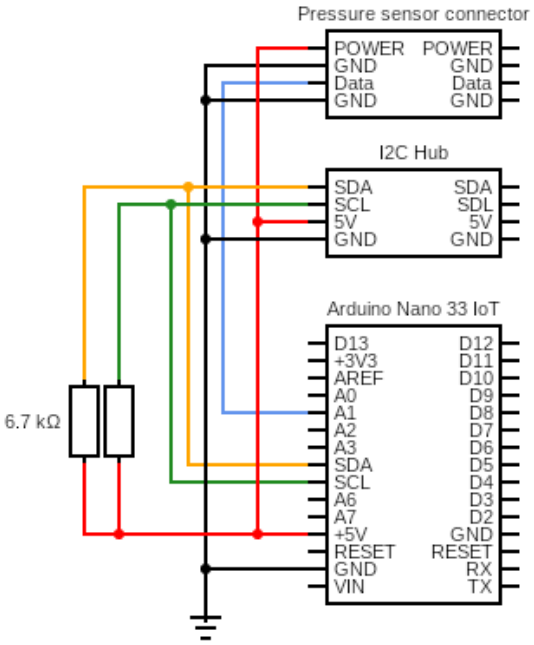

Figure 6: Schematic drawing of connections.

3.3 Software for data collection

The Arduino runs on a C-based programming language and has an extensive repository of libraries available to simplify the process of creating a program. For the flow sensor, the library provided by Sensiron was used without any changes. For the temperature sensors however, the library provided by M5Stack proved difficult to use, and thus custom functions had to be created that could read the binary values outputted by the KMeterISO, and then converted into decimal values that could be read by the user. This is further explained in section 3.3.1.

The pressure sensor does not support I^2C , as it has no internal controller. This was instead connected to an Analog input of the Arduino. All code for the Arduino is available in the associated GitLab project, in the file `customReader.ino`.

3.3.1 *Reading the temperature*

To read the temperature in Celsius, one first needs to write the code `0x00` to the specific sensor on the correct I^2C address. This allows the microcontroller in the temperature sensor to send data, and this is collected using a 4-byte large read-buffer. The size is 4 bytes since this corresponds to the temperature in Celsius. To make the result easier to read the data is cast to a 32-bit integer, byte-shifted to convert the value to a readable value and lastly divided by 100 to get the correct value as a float. This value is stored in an array, and the sequence is repeated once for every sensor to finally get an array of floats corresponding to the value from each sensor.

3.3.2 *Data processing*

To process the data and visualize it as graphs and both filtered and raw data a self-made MATLAB script was made. Several types of plots could be extracted to analyze the data thoroughly.

3.4 Experiment Method

This section describes how all experiments were conducted to evaluate the behaviour and performance of the carbon canister under various conditions. Each experiment targeted specific aspects, from sensor validation to understanding the dynamic behaviours of the system. Following systematic execution, thorough evaluations and discussions were performed to make informed decisions on the objectives of future tests. This iterative process ensured a methodical and well-informed approach for each test.

As mentioned earlier, the canisters were filled with butane, and table 3 presents relevant data for each canister utilized.

Table 3: Canister data.

Canister	Type	Filled weight [g]	Mass C_4H_{10} [g]	Comment
1	EU	954.30	108.36	-
2	EU	949.42	108.06	-
3	EU	939.74	107.19	-
4	EU	952.92	111.45	-
5	EU	951.17	109.27	-
6	EU	956.43	108.43	-
7	EU	953.15	108.13	-
8	EU	955.10	106.70	-
9	EU	949.01	101.28	-
10	EU	952.67	102.54	-
20	US	2244.32	226.78	Has a pump for leak detection
21	US	1839.12	146.74	Not full from start
22	US	1918.36	225.70	-
23	US	1899.38	219.12	-
24	US	1913.78	217.28	-

To capture the dynamics of the carbon canister and derive precise measurements during each experiment, a setup of sensors and measurement tools was deployed, as displayed in fig. 7. The flow sensor was mounted at the canister inlet where atmospheric air entered the system. Simultaneously, the pressure sensor was installed at the outlet of the canister. The canister itself was placed on the precision scale allowing monitoring of the weight throughout the experiments. To measure internal temperature variations, small holes were drilled into the canister where the temperature sensors then were inserted.

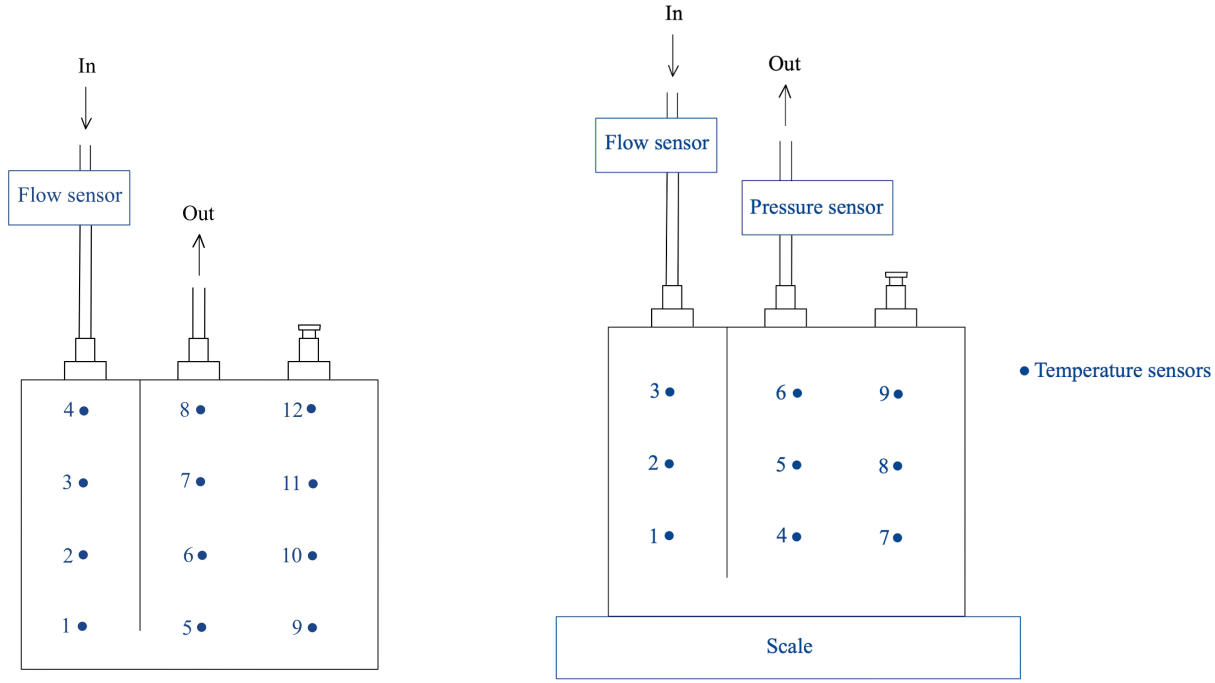

(a) Flow sensor and 12 temperature sensors.

(b) Flow sensor, pressure sensor, scale, and 9 temperature sensors.

Figure 7: Two different sensor layouts for the canister during experiments.

The flow out of the canister was set before each experiment depending on the goal of the experiment. The experiments made are described below.

EXPERIMENT 1 To verify sensor communication, an empty carbon canister was tested. The sensor setup was by fig. 7b with temperature sensors 1-8 and without scale or pressure sensors.

EXPERIMENT 2 To understand the canister's behaviour during purge, an experiment was conducted with a full canister. The sensor setup was by fig. 7b without the scale, pressure sensor, and temperature sensor number 9. A flow of 10 l/min for 20 min was used with canister number 1 was used.

EXPERIMENT 3 To ensure reliable outputs from the temperature sensors, two tests were made where the temperature sensors were compared to a conventional thermometer at room temperature and in a cold environment (freezer).

EXPERIMENT 4 To validate the accuracy of weight measurements for the carbon canister, a digital scale underwent testing. Calibration was performed using a known weight to establish accuracy in weight readings.

EXPERIMENT 5 To investigate mass changes during the purge process, a test with a full canister was made. The test rig was operated with a flow rate of 20 l/min for 40 minutes. Mass measurements were taken every 10 seconds manually throughout the test. The sensor setup was by fig. 7b without the pressure sensor. Canister number 2 was used.

EXPERIMENT 6 To validate the temperature of the canister during the purge process, an experiment similar to Experiment 2 was conducted, but the sensor setup was by fig. 7a but with a scale to weigh the canister. This modification aimed to enhance the resolution of temperature differences within the canister. Mass measurements were taken every 10 seconds manually throughout the test. The test rig was operated with a flow rate of 30 l/min for 40 minutes. Canister number 3 was used.

EXPERIMENT 7 To understand how the canister empties during a normal drive cycle, an experiment was conducted using the FTP-75 drive cycle. The test rig was operated with the purge flow according to FTP75. The sensor setup was by fig. 7b without the pressure sensor, and mass measurements were taken manually before, every 10 seconds throughout the test, and after the experiment. Canister number 4 was used.

EXPERIMENT 8 To validate the functionality of the pressure sensor and scale, a purge cycle was executed with an empty carbon canister. Additionally, the test aimed to gather supplementary temperature and flow data. The test rig was operated with a flow rate of 30 l/min for 40 minutes, The sensor setup was by fig. 7b.

EXPERIMENT 9 To assess the effects of sudden starts and stops in the purge procedure, a test was conducted where the sensor setup was by fig. 7b. The primary goal of this experiment was to gather data specifically related to the abrupt initiation and termination of the purge, as requested by Aurobay. Additionally, the test served a secondary purpose of collecting temperature and flow data. The test rig was operated with a flow rate sequence: 10 l/min for 5 minutes, followed by a 15-minute pause, then 20 l/min for 5 minutes, another 15-minute pause, and subsequently, 30 l/min for 5 minutes, concluding with a 15-minute pause before a final flow of 40 l/min for 5 minutes to halt the procedure. Canister number 5 was used.

EXPERIMENT 10 To evaluate the period required for complete emptying of a filled canister, a test was conducted where the sensor setup was by fig. 7b. The primary objective of this experiment was to attempt to extract the expected mass from the canister but also to generate more data for the model development process. The test rig was operated with a flow rate of 40 l/min for 50 minutes. Canister number 6 was used.

EXPERIMENT 11 To ensure stable and reliable data for model refinement purge cycle was executed at a constant flow rate where the sensor setup was by fig. 7b, and only temperature sensor 1, 3, and 5 was utilized. The purpose of this test was to obtain accurate mass readings of the canister throughout the entire purge duration. The test rig was operated with a flow rate of 30 l/min for 66 minutes. Canister number 7 was used.

EXPERIMENT 12 To gather more data for model refinement, a purge cycle was executed at a constant flow rate where the sensor setup was by fig. 7b, without the pressure sensor and only temperature sensors 3 and 5 were utilized. The purpose of this test was to obtain accurate mass and temperature readings of the canister throughout the entire purge duration. The test rig was operated with a flow rate of 40 l/min for 66.67 minutes. Canister number 8 was used.

EXPERIMENT 13 An experiment with a large canister of US-type. The canister was emptied at a constant flow rate of 40 l/min for 60 minutes. Eight temperature sensors and the scale were used during the experiment. The sensors were put in a configuration as in 7a, the only difference is that the column of sensor 9-12 is not used. Canister number 20 was used.

3.5 Model Method

To create a model of the mass in the canister, the model was initially developed for a stationary flow as this would greatly simplify the parameter fitting. Initially, a model based on eq. (1) was created. In this equation, the flow from

the flow meter was used and the mass was calculated by beginning with the initial mass presented by the scale, and then $\dot{m}_{f,can}$ was added to $m_{f,can}$ for every iteration, giving us a calculated mass at each time instance. The parameter k_1 could then be tuned to fit the measured mass as well as possible. This process was repeated for several stationary flows before it was tested on the FTP75 cycle, which would represent a normal driving cycle.

To further develop the model and capture the dynamic behavior of the mass change a black-box approach was used to extend the model. The extended model can be seen in eq. (7).

$$\dot{m}_{can} = k_1 \cdot \theta \cdot \rho_a \cdot \dot{m}_a + k_2 \cdot \Delta T^2 \cdot \dot{m}_a \tag{7}$$

To find the unknown constants k_1 and k_2 a least squares method was used on equation 7, with the scale mass-difference in each time step as reference. The least squares method utilizes the sum of squares of the residuals to approximate a solution for the unknown constants. The scale mass difference was filtered by calculating the moving average and all positive mass changes were removed since these are considered measurement errors.

4 RESULTS

Several experiments were conducted in alignment with the objectives outlined in section 3. Subsequently, the data obtained from these experiments underwent analysis. The insights gathered from this analysis not only contribute to a deeper understanding of the studied phenomena but also serve as a foundation for planning and executing additional experiments, aimed at exploring other crucial aspects.

4.1 Experiments

The results will cover experiments executed for sensor verification and communication. Relevant results from the purging experiments will be displayed.

4.1.1 *Experiment 1, 3, 4, 8*

The execution of Experiment 1, aimed at verifying the sensor communication for the temperature and inlet flow, proceeded successfully.

In Experiment 3, designed to ensure reliable outputs from the temperature sensors, both tests conducted yielded positive outcomes. The temperature sensors demonstrated consistency and accuracy.

The validation of weight measurement for the carbon canister, conducted in Experiment 4 using a digital scale was also successful.

Experiment 8 was only made to verify the newly implemented pressure sensor and thus no data was recorded. Some adjustments to the measuring system were made to calibrate the sensor to read the correct pressure.

4.1.2 *Experiment 2 (Canister 1)*

Experiment 2 was the first test which used a canister filled with butane, this was used to verify that the setup worked. This experiment used eight temperature sensors and one flow sensor. The result can be seen in fig. 8.

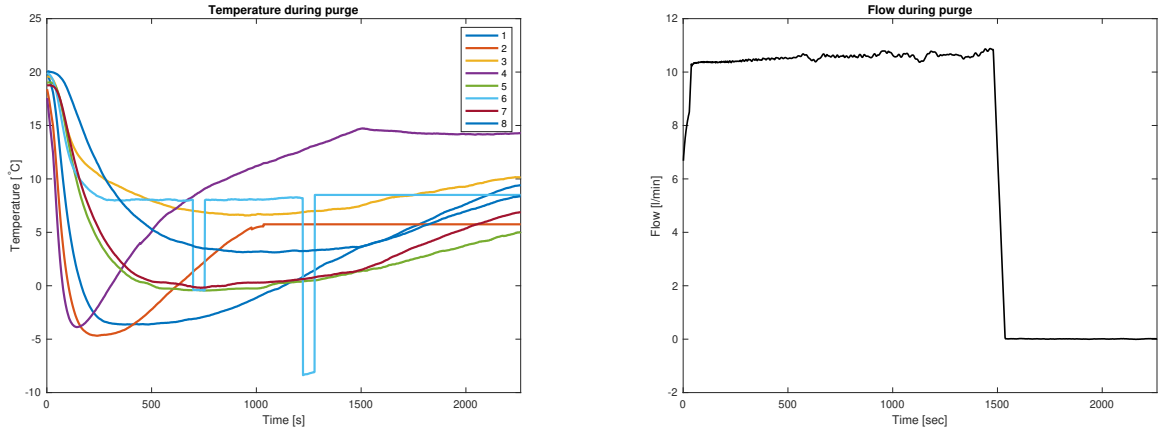

(a) Temperature

(b) Flow

Figure 8: Temperature and flow measurement for experiment 2.

As can be seen from fig. 8a several of the sensors disconnected during the cycle at different times, this is not corrected for.

4.1.3 *Experiment 5 (Canister 2)*

Experiment 5 was executed with a constant flow of 20 l/min for 40 minutes. Canister 2 was used during the experiment, filled with 108.06 g of butane. The mass decreased by 52.7 g and therefore the canister was emptied by 48.77%.

The mass was sampled by hand, with one sample per 10 seconds for Experiment 5. To simplify the modeling this was interpolated to give one measurement every second. The results are shown in fig. 9 and as can be seen some measurement errors occurred because of the instability of the weight measurement setup.

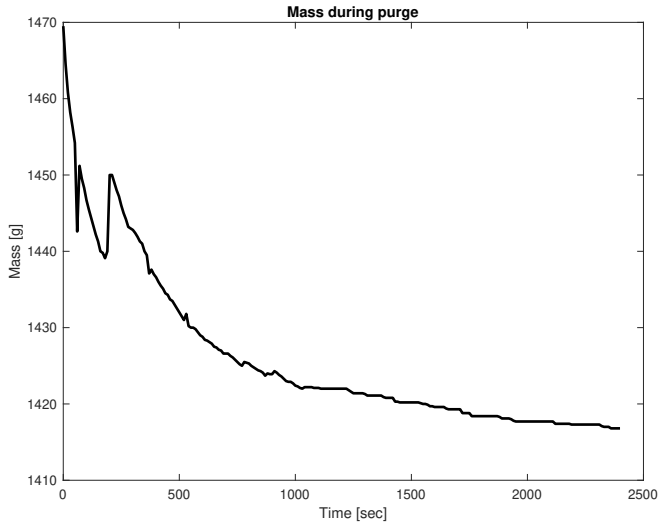

Figure 9: Mass measurements for experiment 5.

4.1.4 *Experiment 6 (Canister 3)*

Experiment with a constant flow of 30 l/min for 40 minutes.

MASS Canister 3 was used during the experiment, filled with 107.19 g of butane. The mass decreased by 50.9g and therefore the canister was emptied by 47.49%. The mass was measured every 10 seconds, and the data was interpolated to simplify modelling.

TEMPERATURE Temperature 1 and 8 send data to the Arduino, but the data is not correct and should therefore not be used. Temperature 7 disconnects after approximately 10 minutes, this is not corrected for. Temperature 2 disconnects after 25 minutes, this is not corrected for either. The sensors disconnecting is probably due to a low baud rate and high measurement frequency, this is changed in the next measurements. The results, without compensating for above mentioned errors, are shown in fig. 10.

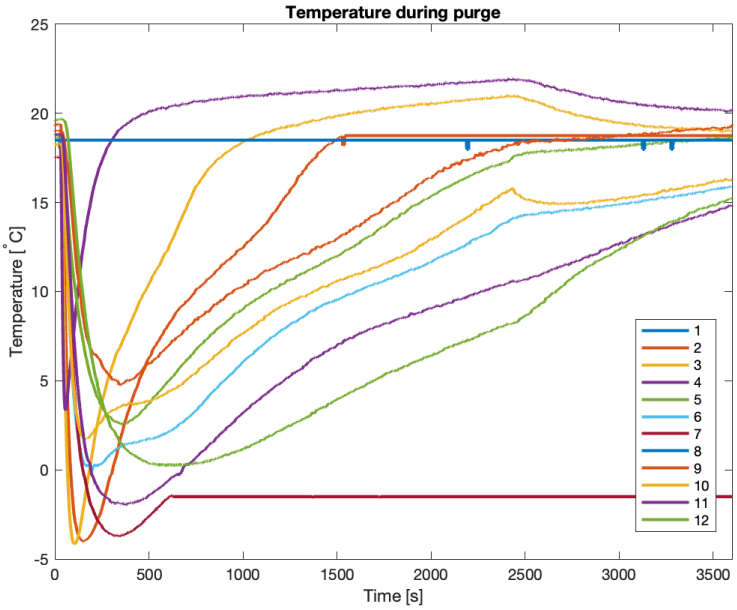

Figure 10: Temperature measurements for experiment 6.

4.1.5 *Experiment 7 (Canister 4)*

Experiment with a varying flow according to an FTP75 drive cycle.

MASS Canister 4 was used during the experiment, filled with 111.45 g of butane. The mass decreased by 32.4 g and therefore the canister was emptied by 29.07%. Below in fig. 11 the measured mass change during the cycle is presented. The sections in the graph where the derivative remains zero come from the purge valve being closed and thereby no air flows through the canister.

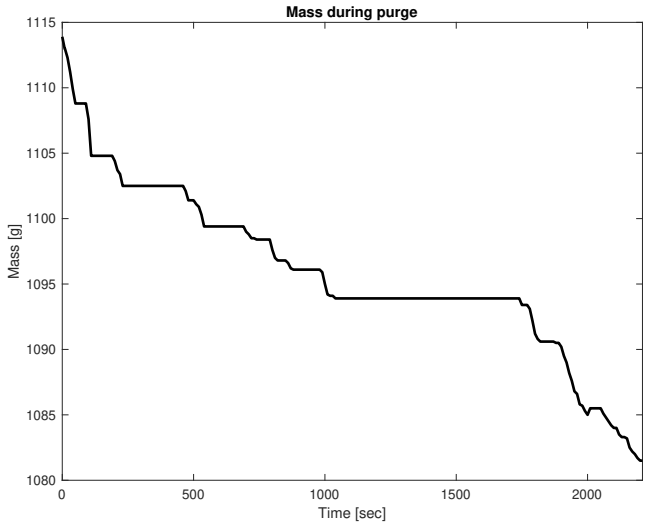

Figure 11: Mass measurements for experiment 7.

TEMPERATURE Temperature was measured using eight temperature sensors, the setup was as in fig. 7b but sensor 9 was not connected. One can see in the figure how the flow moves inside the canister. The temperature quickly decreases to almost $-5°C$ at the first sensor (sensor 3) seen from the "ambient port". As time progresses, the temperature increases for the same sensor. This trend can be seen for all sensors, however, at different times. The times often correlate to how far the flow has to traverse before reaching the sensor.

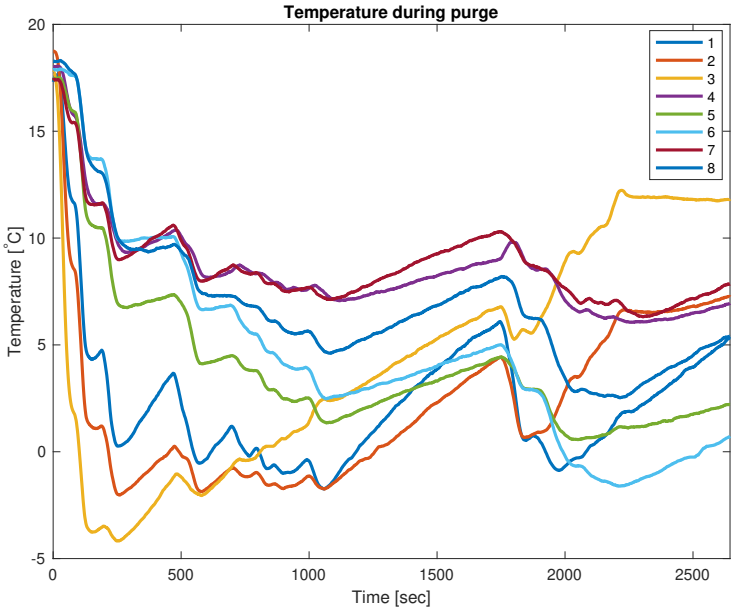

Figure 12: Temperature measurements for experiment 7.

FLOW FTP75 is used to simulate a normal driving cycle, and thus the flow varies quite a bit, as can be seen in fig. 13. Data for the FTP75- cycle was provided by Aurobay.

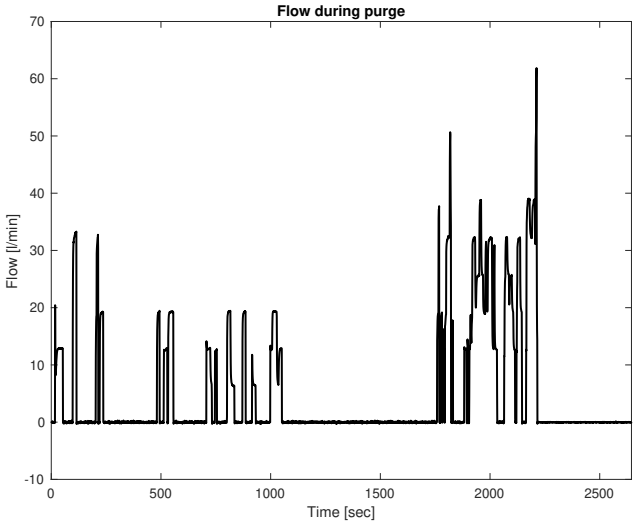

Figure 13: Flow measurements for experiment 7.

4.1.6 *Experiment 9 (Canister 5)*

This experiment was conducted in a start-and-stop fashion where a constant flow was followed by a break then a new flow was applied. The flows used were 10, 20, 30 and 40 L/min.

MASS Canister 5 was used during the experiment, filled with 109.27g of butane. The mass decreased by 45.5g and therefore the canister was emptied by 41.64%. The scale started a self-calibration program during the cycle, and thus some data is missing somewhere after 2500 seconds.

Figure 14: Mass over time for Experiment 9.

TEMPERATURE In fig. 15 the temperature over time can be seen. The dotted vertical lines represent a switch between purge and no purge, the smaller areas between the lines are during purge. As seen by the figure, temperatures decrease as a flow is introduced to the canister, and increase as the flow is shut off.

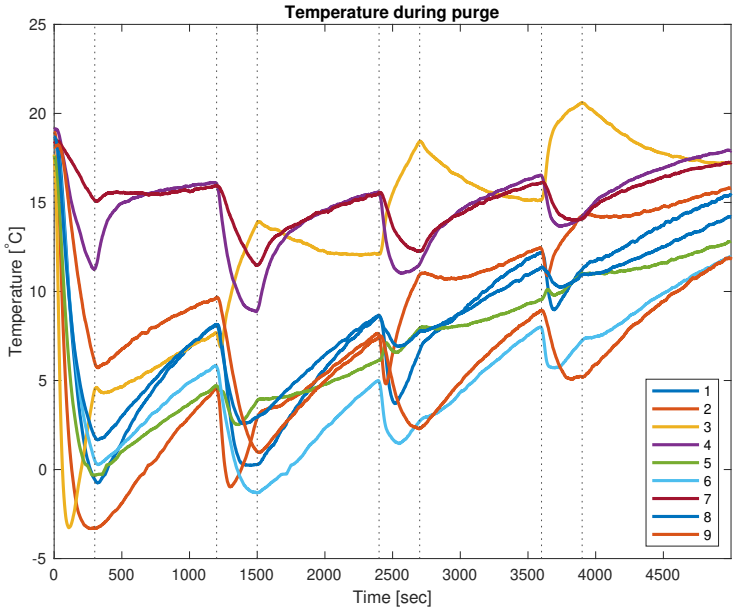

Figure 15: Temperature measurements for experiment 9.

PRESSURE AND FLOW Measured flow and pressure are illustrated in fig. 16. These are presented in the same plot to show that there seems to be some correlation between flow and pressure.

The pressure in the canister, p, is exclusively measured in Experiment 9 (Canister 5). However, based on the findings from that experiment, it is observed that the pressure in kPa closely approximates -1/10 of the flow. Consequently, a straightforward model for canister pressure, in bar, is formulated for cases where the pressure is unmeasured, as illustrated in eq. (8).

$$P = 1.01325 - \frac{\dot{m}_a}{100} \tag{8}$$

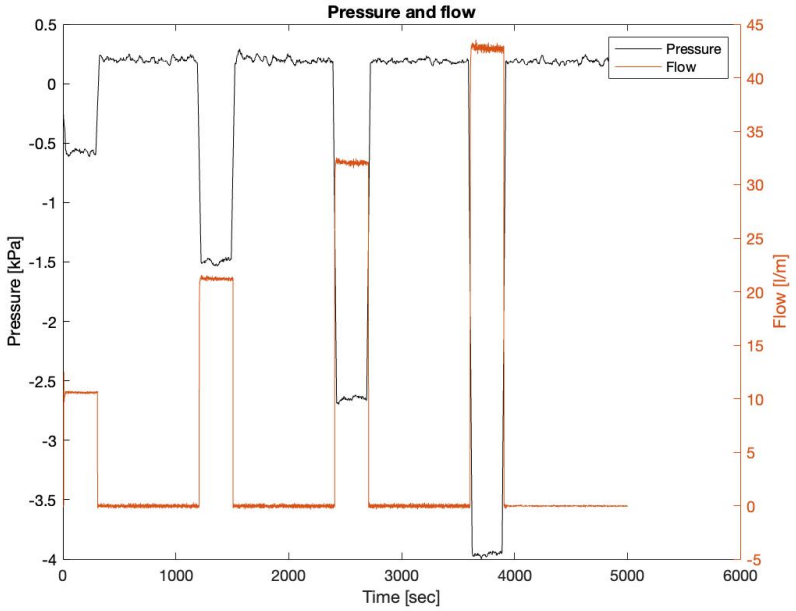

Figure 16: Pressure and flow measurements for experiment 9.

4.1.7 *Experiment 10 (Canister 6)*

The experiment was conducted with a constant flow of 40 l/min for 50 minutes. Sensor communication problems prevented all measurements via the Arduino. The experiment provided data for the mass and the outlet flow from the canister, obtained from Aurobays test bench.

MASS Canister 6 was used during the experiment, filled with 108.43 g of butane. The mass decreased by 100.2 g and therefore the canister was emptied by 92.41%. In fig. 17 the measured weight during the purge procedure is shown. The small increase of mass at approximately 1600 seconds is an effect of external disturbance on the scale during measurements, the mass should normally not increase during the cycle.

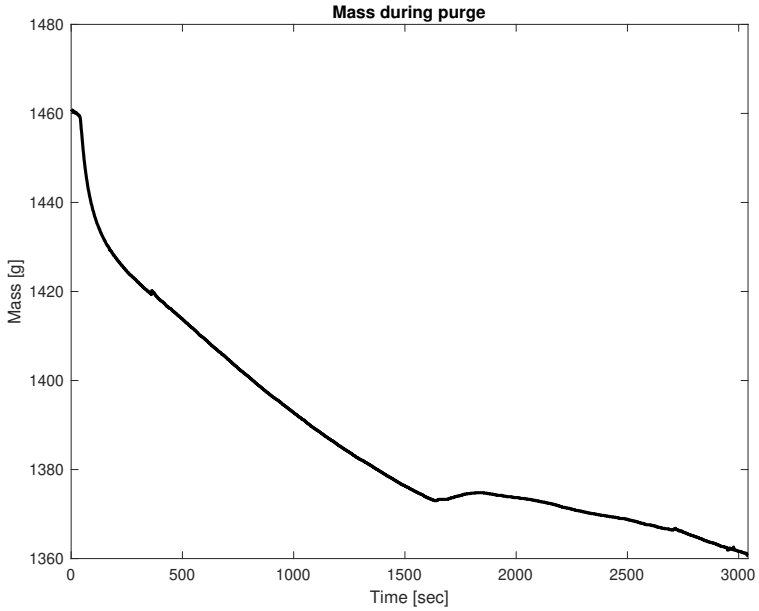

Figure 17: Mass measurements for experiment 10.

4.1.8 *Experiment 11 (Canister 7)*

Sensor communication problems prevented measurements of the temperature, flow into the canister, and pressure. The experiment provided data for the mass and the outlet flow from the canister, obtained from Aurobay's test bench. The experiment was conducted with a constant flow of 30 l/min for 66 minutes. The goal was to collect better data for the model, using a constant flow. No graphs are shown as they do not provide any new results.

Canister 7 was used during the experiment, filled with 108.13 g of butane. The mass decreased by 86.7 g and therefore the canister was emptied by 80.18%.

4.1.9 *Experiment 12 (Canister 8)*

Sensor communication problems prevented measurements of the flow into the canister. The experiment provided data for the temperatures, mass, and outlet flow from the canister, obtained from Aurobay's test bench. The experiment was conducted with a constant flow of 40 l/min for 66 minutes. The goal was to collect more data to be used for the model, therefore there are no graphs shown as they do not provide any new results.

Canister 8 was used during the experiment, filled with 106.7 g of butane. The mass decreased by 90.4 g and therefore the canister was emptied by 84.72%.

4.1.10 *Experiment 13 (Canister 20)*

This experiment provided data for a constant cycle for a US-specified canister and all relevant data could be saved and used for testing of the model. The test was conducted for 60 minutes at a flow of 40 l/min.

MASS Canister 20 was used during the experiment which was filled with 226.8 g of butane. The mass decreased by 186.9 g and therefore the canister was emptied by 82.41%. fig. 18 the measured weight during the purge procedure is shown.

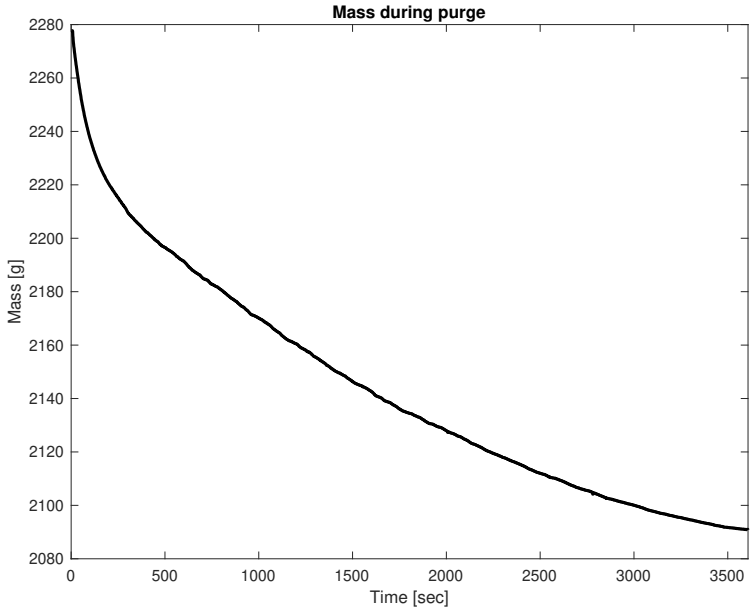

Figure 18: Mass measurements for experiment 13.

TEMPERATURE In fig. 19 the temperature over time.

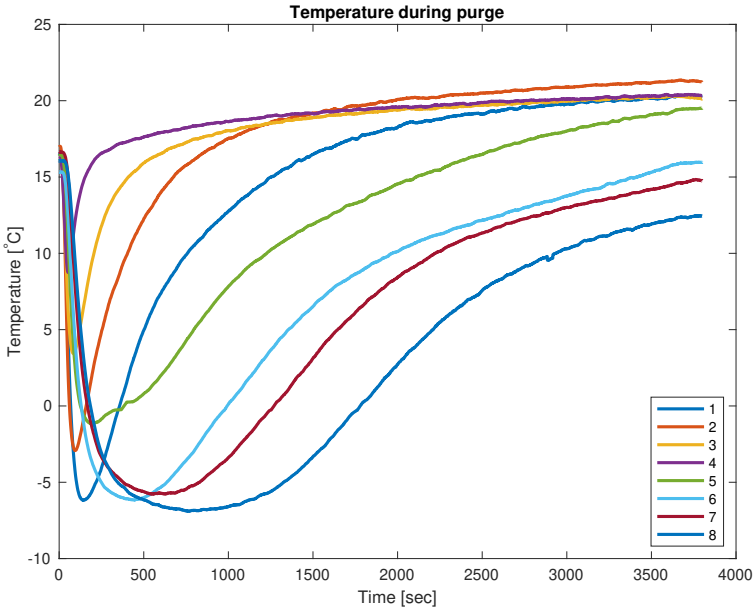

Figure 19: Temperature measurements for experiment 13.

4.2 Model

Throughout this section, the model and how it was derived will be discussed.

4.2.1 *Model based on concentration*

When implementing the model presented in eq. (4) for Experiment 12 (Canister 8) in MATLAB, and adjusting the value of k to accurately predict the final value in the cycle we get the result as in fig. 20. The initial value of the model is set to the initial value of the scale measurement.

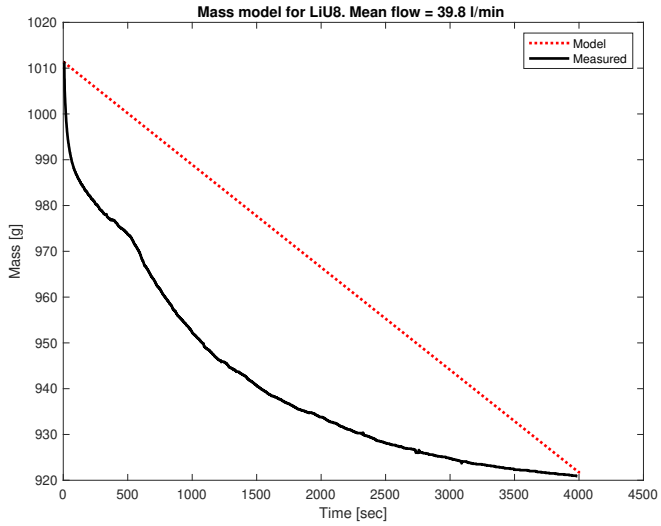

Figure 20: Model based on concentration, constant flow.

From fig. 20 we see that the model performs quite poorly, the figure shows a value of $k = 0.027$. If we, however, test the model on a much more realistic case, the FTP75 cycle, the results are as can be seen in fig. 21.

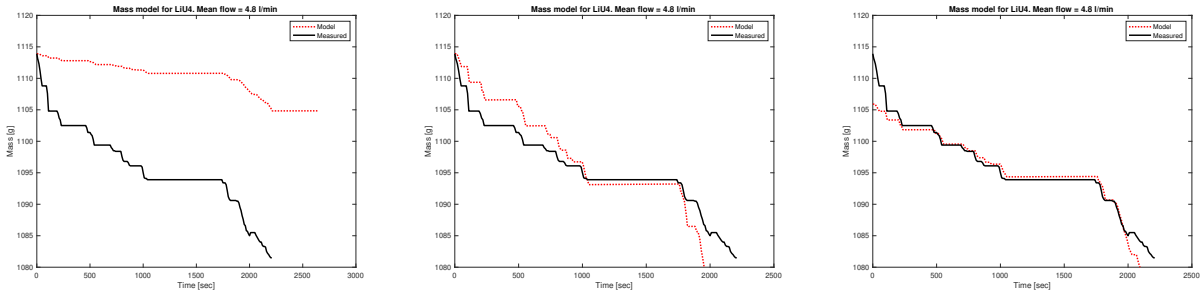

(a) $k = 0.027$ **(b)** $k = 0.18$ **(c)** $k = 0.1$, initial offset = -8 gram

Figure 21: Model performance for different values of k and initial masses on FTP75.

The results in fig. 21 show very good results with a correctly set initial mass and value of k.

4.2.2 *Extension using black-box*

The model introduced in section 3.5, from eq. (4) was extended to give eq. (7). By using the least squares method the values of k_1 and k_2 were calculated. The model was used with the found values and the result can be seen in fig. 22. In fig. 22b, vertical dotted lines represent a break where a new optimal value of k_1 and k_2 has been calculated. This is done as the model performs worse in the beginning, and thus one theory is that optimizing on smaller intervals here is better.

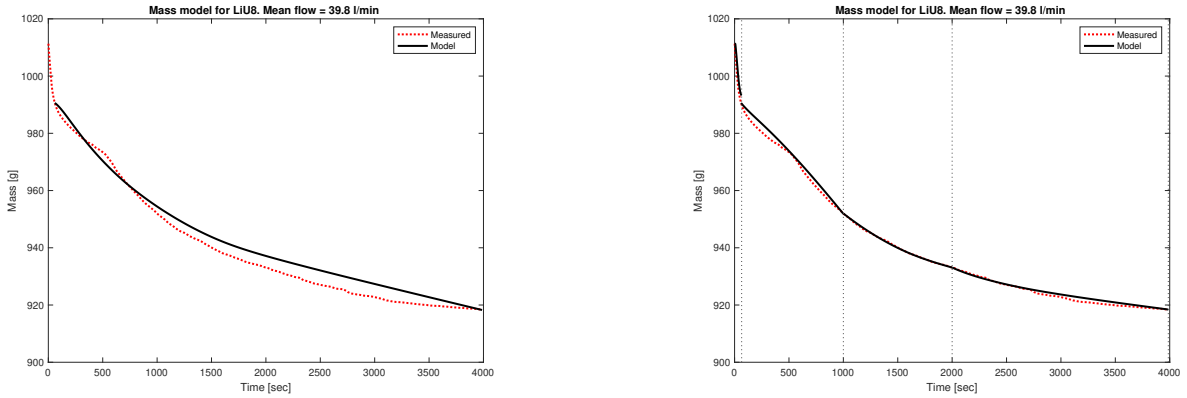

(a) Without intervals

(b) With three intervals

Figure 22: Model performance with and without intervals

From fig. 22 it stands clear that dividing the graph into intervals improves the performance. When applying the model on the FTP75 cycle the results can be seen in fig. 23.

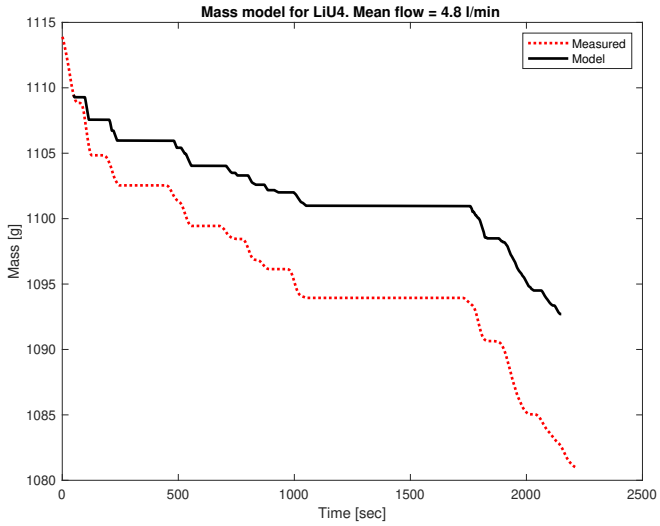

Figure 23: Black box model on FTP75 cycle

4.3 Least squares approximation

The least squares approximation utilizes the residuals of the mass change to find the optimal values of k_1 and k_2. In fig. 24 the measured and model residuals can be seen for a constant flow of 40 L/min (fig. 24a) and the FTP-75 cycle (fig. 24b). As can be seen for the FTP-75 cycle there is a large variety in the residuals, compared to the stationary case.

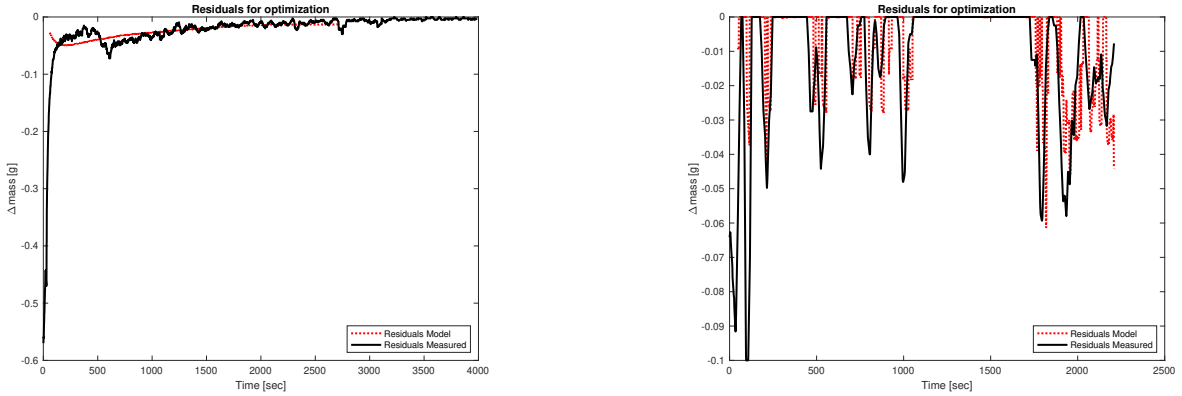

(a) Residuals for a constant flow of 40 l/min.

(b) Residuals for the FTP-75 cycle.

Figure 24: Residuals used in the least squares approximation.

4.4 Mapping optimal k-values

The model used in fig. 22 proves to be good for constant flows, but from fig. 23 it stands clear that the optimization to find the optimal k-values performs much worse on varying flows. Therefore, a mapping is performed on different constant flows which can be used in the model in place of the optimization from section 4.3. The mapping is done in two parts, one for the first minute and one for the rest of the cycle, to capture the initial behaviour. The result is shown in table 4.

Table 4: Values for k during different flows

Flow [l/min]	**0 - 60 seconds**		**60 - ∞ seconds**	
	k_1	k_2	k_1	k_2
20	1.0633	0.00078783	-	-
30	0.71311	$7.2847 \cdot 10^{-5}$	-	-
40	0.55439	$4.7336 \cdot 10^{-5}$	$11.055 \cdot 10^{-3}$	$-1.8848 \cdot 10^{-6}$

For the 20 l/min measurement no suitable values for k_1 and k_2 were found using the least-square optimizer. For the 30 l/min measurement, there was not enough data available to get a value.

5 DISCUSSION

The project has several goals for the system that are to be fulfilled. In the first part of this section, the results from testing the fulfilment of the goals are discussed. Secondly, the implementation and usage of the sensors will be discussed. Lastly, the performance of the model and how it was constructed will be discussed.

5.1 Modeling the flow of hydrocarbons from the canister

The main purpose of the project is to find a model for the flow of hydrocarbons from the charcoal canister. Throughout this section, the model obtained will be discussed.

5.1.1 *Flow from concentration*

By using eq. (4) to model the flow of hydrocarbons, and then using eq. (5)-(6) to calculate the concentration, one gets a model with only one parameter that needs to found, denoted as k_1.

5.1.2 *Parameters from experiments*

As mentioned in section 2.4 the parameters E and n are decided from experiments. By comparing what values used in this report, calculated by Östermark [15], with the values from another article, in this case by Möller [19], we get the two sets of parameters presented in table 5.

Table 5: Parameters for comparison of models.

Parameter	Set A	Set B
E	18422	30179.39
n	1.43	2.84

By running two separate simulations with the two sets of parameters in table 5 and comparing the model output, one can see that the difference between the two sets doesn't have a big impact on the model performance. The result can be seen in fig. 25.

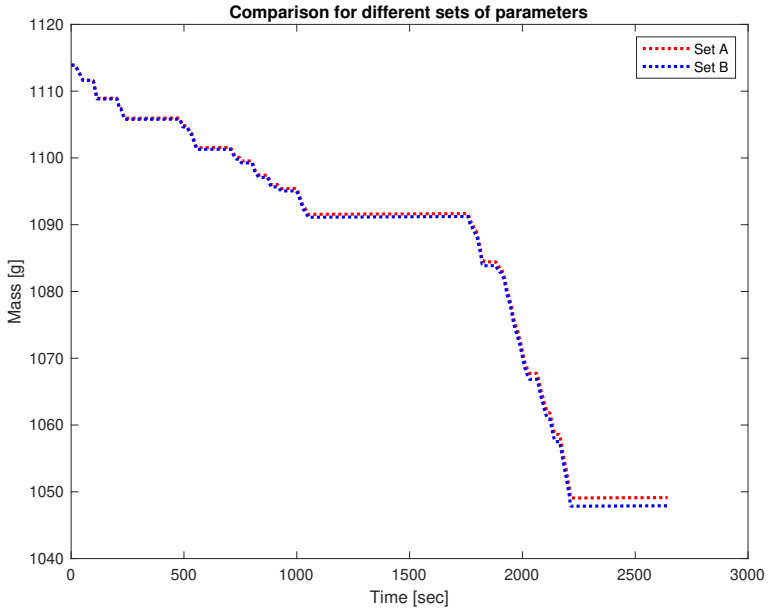

Figure 25: Evaluation for model parameters.

As shown in fig. 25 the two sets give very similar results, and thus it seems reasonable not to investigate what parameters give the best model at this time.

5.1.3 *Available research*

Most of the research available does experimentation and simulations during stationary conditions, no research found investigates dynamic driving cycles, such as the FTP-75 cycle. Thus, the models found in the literature are in most cases not applicable to dynamic cases as they consider many variables as constant.

5.2 Purge airflow

The purge flow through the canister shall not exceed 1.5 g/s. This can be converted to litres per minute by using the density of air at $20^{\circ}C$ at standard atmospheric pressure (1.013 bar), which is 1.204 kg/m^3. The calculations can be seen below.

$$V = \frac{0.0015 \text{ kg}}{1.204 \text{ kg}/m^3} \approx 0.00125 \ m^3.$$

Since 1 liter is 0.001 m^3 the volume can be converted to liters as follows.

$$V = \frac{0.00125}{0.001} = 1.25 \text{ L}.$$

Therefore, the airflow through the canister shall not exceed the calculated flow of 1.25 L/s or 74.75 L/min.

5.3 Hydrocarbon flow from the canister to the engine

The limitation on the hydrocarbon flow from the canister to the engine is to not exceed 30% of the total fuel flow to the engine, the following subsections verify that this requirement is met.
To evaluate the performance requirements on the model a rough estimate of the fuel consumption of a car is used. This is because there is no car to experiment and measure from. The estimation used for a regular car is $0.6\frac{L}{10km}$. The fuel consumption is compared with the calculated fuel consumption from the FTP-75 driving cycle. The total fuel consumption for a regular car on the FTP-75 drive cycle is below $V_{tot,petrol}$.

$$V_{tot,petrol} = 17.77km \cdot 0.06\frac{L}{1km} = 1.0662L$$

During the time of the cycle (1369 seconds) the average fuel flow is calculated as follows.

$$\dot{V}_{fuel} = \frac{1.0662 \text{ [L]}}{1874 \text{ [s]}} \cdot 60 \left[\frac{s}{min}\right] \approx 0.0341 \left[\frac{L}{min}\right]$$

Utilizing the density of unleaded 95-octane petrol, which is 750 kg/m^3 or 750 g/l the equation above can be converted as follows.

$$\dot{m}_{\text{fuel, calc}} = 0.00057 \left[\frac{L}{min}\right] \cdot 750 \left[\frac{\text{g}}{\text{L}}\right] \approx 25.60 \left[\frac{\text{g}}{\text{min}}\right]$$

To accommodate the requirement that the flow of hydrocarbons should not exceed 30% of the total fuel flow to the engine, the following calculation was made.

$$\dot{m}_{\text{tot, calc}} = \frac{25.60}{0.7} \approx 36.58 \left[\frac{\text{g}}{\text{min}}\right]$$

$$\dot{m}_{\text{hydrocarbon, lim}} \leq 0.3 \cdot \dot{m}_{\text{tot, calc}} \approx 10.97 \left[\frac{\text{g}}{\text{min}}\right]$$

This means that the flow of hydrocarbons should not exceed 10.97 $\frac{\text{g}}{\text{min}}$.

To verify the requirement that the maximum fuel used from the canister for combustion does not exceed 1.5 g/s the purged fuel was calculated using the measurement data. The data from section 4.1.5 Experiment 7, of the FTP-75 was used to calculate the flow of hydrocarbons. This can be seen below.

$$\dot{m}_{\text{hydrocarbon, act}} = \frac{m_{\text{emptied, HC}}}{t_{FTP}} = \frac{32.4[\text{g}]}{1874[s]} \approx 1.0372 \left[\frac{\text{g}}{\text{min}}\right] \tag{9}$$

When compared to the limit calculated as $\dot{m}_{hydrocarbon,lim}$ it can clearly be seen that $\dot{m}_{\text{hydrocarbon, act}} < \dot{m}_{\text{hydrocarbon, calc}}$ and therefore the requirement is fulfilled.

5.4 Precision of hydrocarbon flow estimation

There are two goals for the precision of hydrocarbon flow estimation. During a transient the precision should be a maximum of 5% of the total fuel flow. In stationary, it should instead be 1% of the total fuel flow.

To show that the transient of under 5% requirement is met, the following graphs are evaluated:

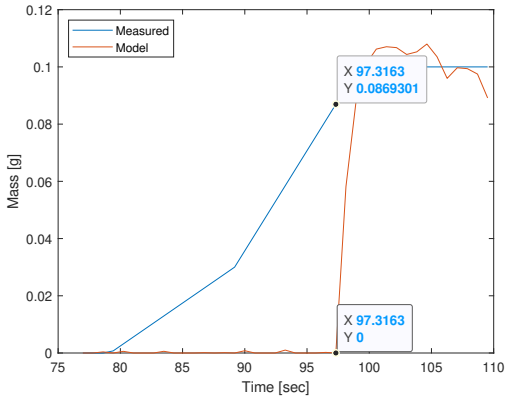

(a) Residuals for the FTP-75 cycle

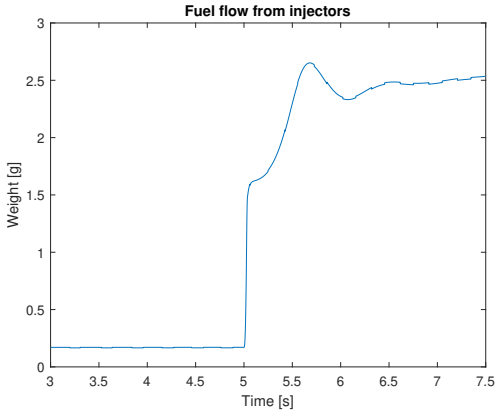

(b) Fuel flow for an arbitrary engine with a step in gas pedal position from 10% to 80%

Figure 26: Residual transients compared

From these plots, the following fuel flows can be derived (in a transient):

Flow	Value
Canister flow, measured	0.086 g/s
Canister flow, model	0 g/s
Difference	0.086 g/s
Injector fuel flow	2.5 g/s
Total fuel flow	2.586 g/s
Difference in percentage	3.33%

Table 6: Percentage of residual differences

To show that the constant case does not exceed 1% of error the following graphs are studied:

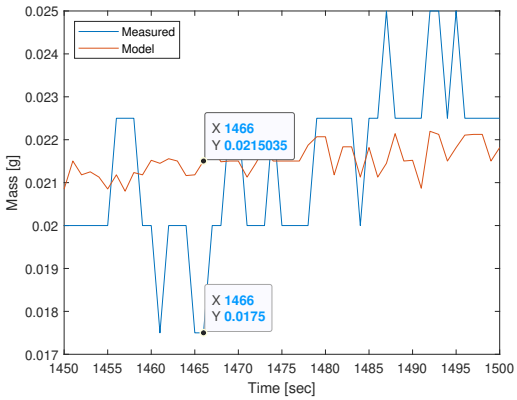

(a) Residuals for a constant flow of 40l/min

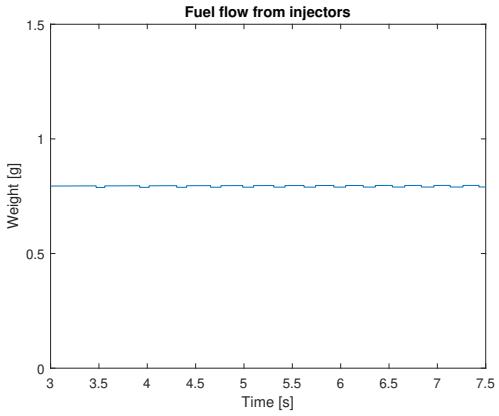

(b) Fuel flow for an arbitrary engine with a constant gas pedal position of 30%

Figure 27: Constant transients compared

From these plots, the following fuel flows can be derived (in the constant state):

Flow	Value
Canister flow, model:	0.021 g/s
Canister flow, measured	0.018 g/s
Canister flow, difference	0.003 g/s
Injector fuel flow	0.69 g/s
Total actual fuel flow	0.708 g/s
Difference in percentage	0.43%

Table 7: Percentage of residual differences in the constant state

As can be seen from the graphs and calculations above, these requirements are met.

5.5 Measurement error occurrence

In the course of the experimental procedure, measurement errors were encountered, particularly for the stability of the weight measurements. The time required for the scale to achieve stability consistently increased, likely due to sub-optimal setup conditions with loose cables, hoses, and sensors.

Inconsistencies were noted in Experiment 10 (Canister 6) and Experiment 12 (Canister 8), where the flow rate was set to 40 l/min for 50 minutes and a duration of 66 minutes, respectively. The canister was emptied to a higher percentage in the shorter experiment, whereas it should have been more depleted in the longer one. Several variables may influence these results, including variation in the measuring faults in the lab setup. This is mostly due to the canister being unstable on the scale during the experiments and some small faults with the other sensors. The local grain size of the carbon pellets inside of the canister is another factor that could have an impact on these inconsistencies.

The logging of temperatures and flow into the canister froze or abruptly stopped during the execution of certain experiments, resulting in data loss. This issue was particularly evident when using more than 9 temperature sensors and also when the pressure sensor was implemented. Possible causes for this include that the lab equipment had small sudden voltage drops for a particular sensor. Another cause is that the Arduino could not support that amount of sensors for a longer time.

5.6 Implementation of temperature sensor

In a real-life scenario, it is recommended from the observations that a temperature sensor is permanently installed in the carbon canister. What can be seen from the experiments is that it should be placed in the middle of the canister, sensor number 5 in fig. 15 and fig. 12. This recommendation can be verified by the following graph:

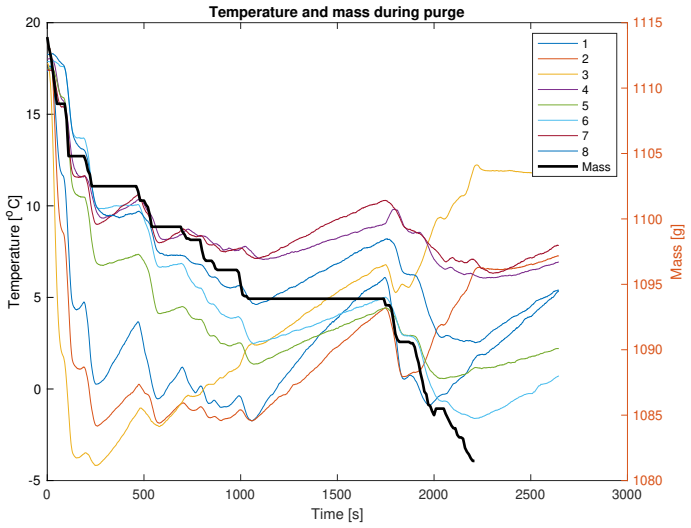

Figure 28: Mass and temperature in the same graph where temperature sensor 5 follows the dynamics in the mass the best.

In this case, the sensor is placed in position 5 in layout **(b)** from fig. 7 i.e. in the centre of the canister. To capture the dynamics from the purge inside the canister it can be seen in fig. 28 that this position of the sensor follows the derived model best. This is therefore a recommendation for a suitable placement.

5.7 Implementation of flow

A flow sensor is a relatively expensive sensor to add to a mass-produced vehicle. This means that the flow input signal needs to be derived from elsewhere. This could be done by using section 5.7 and the pressure sensor at the intake manifold to calculate the pressure at the canister. The pressure can then be used to easily calculate the flow through the canister. The calculation needs the data and dimensions of the intake manifold pressure, ambient pressure, pipe diameters, and lengths between the canister and intake manifold. This could then be used to estimate the flow at the

canister and be used in the model.

An alternative approach, though deemed less optimal, could also be to implement a dedicated pressure sensor for the canister and use eq. (8) to calculate the flow from the pressure difference.

$$q_m = C \cdot A_2 \sqrt{2\rho(p_1 - p_2)} \tag{10}$$

Where q_m is the mass flow through the canister, C is a dimensionless constant, A_2 is the orifice cross-section area, ρ is the density of the air and p_1 and p_2 is the upstream- and downstream pressure.

5.8 Model Performance

When evaluating the first model from eq. (1) on the test data, the results were inconclusive. When using the model to estimate the mass difference during the FTP-75 cycle one can tell that the overall behavior of the model fits well with the measured mass. However, there is a large offset between the two, which can be seen in fig. 21a. However, when using the model on a constant flow experiment it completely misses the dynamic behavior of the mass change. When evaluating the model closer it was found that all input variables were somewhat linear, resulting in a linear behaviour on the model mass change, fig. 20. To compensate for this and find a more dynamic model a black-box method was used to extend the model. Through further discussions and evaluation of the measurement data, it was found that the temperature in the carbon canister could have a greater impact on the purged carbon volume than earlier thought. From this conclusion, several extensions of the model were generated and evaluated on the FTP-75 cycle. The final model can be seen in eq. (7) where the temperature difference during purge was used, a constant k_2, and the measured flow. The flow was only implemented to stop the mass change when the purge valve was closed. This is because the temperature increases when there is no purge. When evaluating this extended model on the constant flow case one can tell that the results are much more promising. The results are promising when comparing the extended model with the measurement data in fig. 22a. The model can estimate the mass change well and the least squares method can find suitable values for the constants k_1 and k_2 to fit the model.

5.9 Usage of least squares approximation

To find the correct values on the constants k_1 and k_2 a least squares approximation was used on the residuals of the mass change. The residuals were filtered and all positive residuals were removed since they originated from measurement errors during purging, i.e. it is not reasonable for the mass to increase during purge. The filtering of the residuals was executed by calculating the moving average, to remove any inconsistencies in the data. When studying the resulting residuals with the calculated change of mass for the FTP-75 cycle in fig. 24b it is clear that the data used in the least squares method don't show a consistent behaviour. However, when using a constant flow the residuals show a more linear behaviour, as can be seen in fig. 24a. This enables the least squares approximation to find better suitable constants and by that a better model. To further enhance this the residuals can be divided into several groups where an optimal value for the constants can be found. The issue with this approach is that the mass decreases drastically when the purge is started. This behaviour is often missed when using the least squares approximation on the whole experiment time. Since the question to be answered is to model this behavior the constants for the first 60 sec of each measurement were calculated. These constants work badly for the whole cycle but capture the first 60 sec of the behaviour well.

6 CONCLUSION

In conclusion, this report has provided a comprehensive overview of the experiments conducted to analyze the purge cycle of carbon canisters in the context of forecasting carbohydrate purging. Data from the experiments were acquired with a measuring rig, utilizing a Raspberry Pi, an Arduino and several sensors including flow, pressure, temperature and a scale. The investigation involved two different canister sizes utilizing purge, contributing to a deeper understanding of the system behaviour.

Parallel to the experimental phase, significant strides were made in the development of the canister model. The model evolved together with the increasing datasets, acknowledging behaviours between input signals and demonstrating a dedication to ongoing enhancement.

The first two goals presented under section 1.3 have been fulfilled, the laboratory equipment is in working condition and has a user manual to allow external users to operate the setup. Furthermore, a model has been presented to model the flow of hydrocarbons through the canister. The goal of regulating the EVAP flow for arbitrary purging has not been investigated due to a lack of time. Because of this, the two goals regarding using the regulator and demonstrating it on a real engine have not been further investigated.

Finally, the key takeaway from this project is the following:

1. A more robust and reliable setup should be developed to reduce the measurement errors and disturbances that affect the measurement data.
2. More measurements need to be made since the Arduino proved to be unreliable and because of this a lot of data got lost.
3. If a temperature sensor is to be implemented this should be done either in the middle of the carbon canister or close to the tank inlet.
4. To model the flow through the canister, the already implemented sensors in the vehicle should be used to the largest extent.
5. There is no one size fits all for a model, the report has presented one model together with some tuning parameters for a few constant flows.

7 FUTURE WORK

The following section presents some suggestions for future work and wisdom gained during the project. How the project could have been conducted more smoothly and what extensions could be made. This is primarily to assist the reader who intends to continue working on this subject.

7.1 Data collection

Early on in the project, much time was spent on data collection and sensor communication, to collect data to help create a model. This did however prove to be quite hard, and the setup for data collection has quite a few flaws. For unknown reasons, the logging freezes from time to time. When this happens the measurement data is completely removed. Future work should therefore explore the possibility of creating a more stable setup for the data collection, as this could greatly reduce the time required for test and also lay the foundation to create a more accurate model.

7.2 Laboratory setup

To retain more accuracy in the measurements the laboratory setup should be extended. To minimize any external influence during the purge experiments the laboratory setup should be extended to where all sensors, hoses, and cables can be fastened. This is especially important when measuring the weight of the canister since the change of mass during purge is a tenth of a gram in size. This enables much room for error where the slightest shifting or movement of the connections has a large impact on the measurements. To further organize the laboratory setup a trolley similar to the grey box setup could be used where all components could be fastened and standardized connections could be used.

During this project, the experiments have only been conducted on the purging of the canister. In section 2.1 the problem of high concentrations of hydrocarbons at critical locations inside the canister is mentioned. An idea for improvement would be to connect a tank containing hydrocarbons to the canister. With this kind of setup, the emptying of the canister would be closer to reality. This would make the purging more realistic and a better representation of the fumes that enter the canister from the gas tank and a more accurate representation of the purge system.

7.3 Modeling

A model that can be implemented if all measurements are in place, is a model for a "virtual" flow sensor to predict the flow in the canister. This can be done through a derivation from the intake manifold pressure to the canister pressure.

Another aspect that could have been added to the model is the impact of different surrounding temperatures and air pressures. For example driving at high altitudes where the air pressure is lower and the temperature often is lower, as opposed to driving in a city at ground level. The temperature of the engine bay could also have an impact on the adsorption attributes of the carbon and similar aspects.

In a real-world scenario, when the canister is to be emptied during actual driving in a car, it may be desirable to use a different method to determine the parameters for the model. What then could be used is for example a Kalman filter to further develop the model.

REFERENCES

[1] J. O. de Beeck, J. Thompson, and N. Booth, "Upcoming emission regulations for passenger cars: Impact on scr system requirements and developments," SAE Technical Paper, Tech. Rep., 2013.

[2] Naturvårdsverket, "Klimatet och transporterna," 2022, [Online; accessed 9-November-2023]. [Online]. Available: https://www.naturvardsverket.se/amnesomraden/klimatomstallningen/omraden/klimatet-och-transporterna/

[3] L. Romagnuolo, E. Frosina, F. Fortunato, A. Andreozzi, and A. Senatore, "1d model for n-butane adsorption and thermal variation for evap canister of gasoline-fueled vehicles: Validation with experimental results and dfss optimization," *Applied Thermal Engineering*, vol. 209, p. 118267, 2022. [Online]. Available: https://www.sciencedirect.com/science/article/pii/S1359431122002265

[4] MSB, *Hantering av brandfarliga gaser och vätskor på bensinstationer*. -: Advant Produktionsbyrå, 2015.

[5] R. C. Bansal and M. Goyal, *Activated Carbon Adsorption*. CRC Press, May 2005, google-Books-ID: VUluB-wAAQBAJ.

[6] Q. Cao, K.-C. Xie, Y.-K. Lv, and W.-R. Bao, "Process effects on activated carbon with large specific surface area from corn cob," *Bioresource Technology*, vol. 97, no. 1, pp. 110–115, 2006. [Online]. Available: https://www.sciencedirect.com/science/article/pii/S0960852405001094

[7] H. Z. R.V.Mantri, R.Sanghvi, *Developing Solid Oral Dosage Forms (Second Edition)*. Academic Press, 2017.

[8] P. Johnson, D. J. Setsuda, and R. Williams, "Chapter 8 – activated carbon for automotive applications," 1999. [Online]. Available: https://api.semanticscholar.org/CorpusID:107148866

[9] "Nano 33 IoT | Arduino Documentation." [Online]. Available: https://docs.arduino.cc/hardware/nano-33-iot

[10] Raspberry Pi Foundation. (2023-11-07) Raspberry pi 3 model b+. [Online]. Available: https://raspberrypi.dk/en/product/raspberry-pi-3-model-b-plus-2/

[11] "I2C - SparkFun Learn." [Online]. Available: https://learn.sparkfun.com/tutorials/i2c/all

[12] Wikipedia contributors, "I²c — Wikipedia, the free encyclopedia," 2023, [Online; accessed 27-September-2023]. [Online]. Available: https://en.wikipedia.org/w/index.php?title=I%C2%B2C&oldid=1175364246

[13] J. Valdez and J. Becker, "Understanding the I2C Bus," 2015.

[14] A. T. Zaremba and M. Jennings, "Purge Modeling for New Propulsion System Technology Applications," *SAE International Journal of Engines*, vol. 4, no. 1, pp. 998–1006, Apr. 2011. [Online]. Available: https://www.sae.org/content/2011-01-0858/

[15] E. Östermark, "Modelling of a Purge Heated Carbon Canister Using CFD," vol. 2018, p. 87.

[16] C. Nguyen and D. Do, "The dubinin–radushkevich equation and the underlying microscopic adsorption description," *Carbon*, vol. 39, no. 9, pp. 1327–1336, 2001. [Online]. Available: https://www.sciencedirect.com/science/article/pii/S0008622300002657

[17] "Antoine equation," Oct. 2023, page Version ID: 1181087069. [Online]. Available: https://en.wikipedia.org/w/index.php?title=Antoine_equation&oldid=1181087069#cite_note-1

[18] N. O. o. D. a. Informatics, "Butane," publisher: National Institute of Standards and Technology. [Online]. Available: https://webbook.nist.gov/cgi/cbook.cgi?ID=C106978&Units=SI&Mask=1F#:~:text=Antoine%20Equation%20Parameters

[19] E. Möller, "Modelling and Simulation of an Activated Carbon Canister," vol. 2016, 2016.